ISBN: 978-3-95450-168-7 doi:10.18429/JACoW-IPAC2015-MOPWA031

A NEW APPROACH FOR RESISTIVE WAKEFIELD CALCULATIONS IN TIME DOMAIN

A. Tsakanian#, E. Gjonaj, H. De Gersem, T. Weiland, TU-Darmstadt/TEMF, Darmstadt, Germany
M. Dohlus, I. Zagorodnov, DESY, Hamburg, Germany

Abstract

We report on a new numerical technique for the computation of the wakefields excited by ultra-short bunches in the structures with walls of finite conductivity. The developed 3D numerical method is fully time domain. It is based on special Staggered Finite Volume Time Domain (SFVTD) method and has no numerical dispersion in all three axial directions simultaneously. The resistive boundary model applies Surface Impedance Boundary Condition (SIBC) evaluation in time domain and covers boundary effects like frequency dependent conductivity, surface roughness and metal oxidation. A good agreement between numerical simulation and perturbation theory is obtained.

INTRODUCTION

Electromagnetic wakefields due to the finite conductivity of cavity walls are one of the main concerns in the design of electron accelerators. These so called resistive wall wakefields are the largest contributor to beam coupling impedances in the high energy sections of the accelerator where extremely short electron bunches are operated [1]. For an estimation of these contributions one relies (almost) exclusively on numerical simulations, since wakefield measurements within the high-vacuum accelerator chamber are very cumbersome.

Conventional methods for the solution of Maxwell's equations in the time domain, however, will usually fail for this class of problems. This is primary due to the extremely high frequency of wakefields resulting in large numerical dispersion errors. These errors tend to accumulate in the course of the simulation as, e.g., short electron bunches of μm-length propagate over several meters within the accelerator.

To cope with this problem, specialized low-dispersion techniques have been proposed [2]. The SFVTD method introduced in [3] is one of them. It represents a volume-integral based formulation with very appealing numerical properties. The dispersion error of SFVTD is substantially smaller than that of the conventional FDTD technique. The crucial property, however, is that the method can be operated at a maximum stable time step corresponding to the 1D-CFL stability limit. Applying SFVTD at this so called 'magic' time step provides the exact, dispersion-free solution for all electromagnetic waves propagating along the three main axis directions (cf. [3]).

In order to take into account resistive and/or rough wall wakefields in such simulations, however, an appropriate implementation of broadband SIBC for SFVTD is needed. In the following, this task is accomplished by combining the ADE technique with a particular time stepping scheme. This latter allows to maintain the numerical dispersion and stability properties of the original SFVTD which are necessary for this type of simulations.

THE SFVTD METHOD

The basic idea of the SFVTD discretization is depicted in Fig. 1. Fields and currents are allocated component-wise on the faces of a Cartesian mesh. For each of these components a unique control volume enclosing the corresponding mesh face is introduced. Alternatively, one may think of three secondary, staggered meshes which are obtained by shifting the original mesh along the x-, y- and z-directions, respectively.

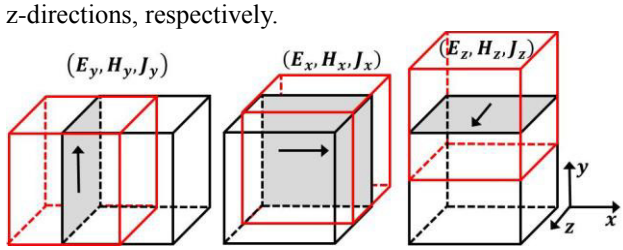

Figure 1: Allocation of fields and currents on mesh cells (black) and corresponding control volumes (red) of SFVTD.

A discretization of Maxwell's equations is obtained by applying the generalized Stokes' theorem for each of the 6 field components on the corresponding control volumes. A detailed derivation of these equations is given in [3]. Here, we begin with the semi-discrete form of SFVTD:

$$\boldsymbol{M}_{\mu}\frac{d\boldsymbol{h}}{dt} = -\boldsymbol{C}\boldsymbol{e}\ , \tag{1}$$

$$\boldsymbol{M}_{\varepsilon}\frac{d\boldsymbol{e}}{dt} = \boldsymbol{C}^{T}\boldsymbol{h} - \boldsymbol{j}\,. \tag{2}$$

In (1), (2), $\boldsymbol{e}$, $\boldsymbol{h}$ and $\boldsymbol{j}$ represent volume averages over the control volumes of the electric, magnetic and current field components, respectively. The matrices, $\boldsymbol{C}$, $\boldsymbol{M}_{\varepsilon}$ and $\boldsymbol{M}_{\mu}$ are the *curl*- and *mass*-operators of the method resulting from this particular choice of integration volumes on the mesh. The particular form of these matrices determines the numerical properties of the SFVTD method such as the low numerical dispersion and the large bound of stability.

In figure 2 are presented the numerical phase velocity behavior of the plane wave versus its propagation direction. Both, SFVTD and conventional FDTD methods are evaluated at their stability limits, i.e. FDTD - $c\Delta t_{2D} = \Delta/\sqrt{2}\,, c\Delta t_{3D} = \Delta/\sqrt{3}$, SFVTD - $c\Delta t_{2D,3D} = \Delta$.

Content from this work may be used under the terms of the CC BY 3.0 licence (© 2015). Any distribution of this work must maintain attribution to the author(s), title of the work, publisher, and DOI.

ISBN: 978-3-95450-168-7 doi:10.18429/JACoW-IPAC2015-MOPWA031

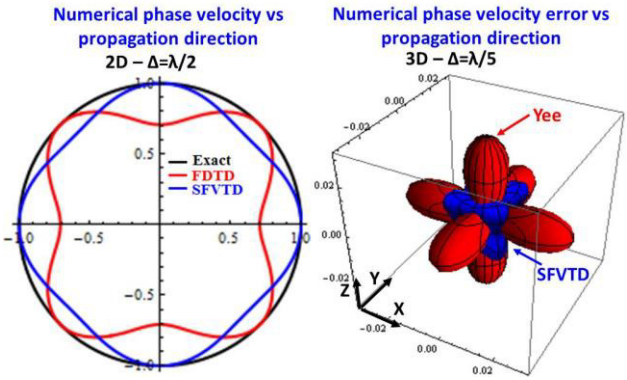

Figure 2: The behavior of numerical phase velocity of FDTD (red) and SFVTD (blue) methods vs plane wave propagation direction.

As can be seen the SFVTD method has no dispersion error along the coordinate axis while the Yee-FDTD scheme is dispersion free along the space diagonals. From other side, already with five discretization points per wavelength the SFVTD method has about 1.7 times better accuracy than conventional FDTD.

TIME-DOMAIN MODEL OF SURFACE IMPEDANCE BOUNDARY CONDITION

In the following, first order Leontovich type SIBC are considered $\boldsymbol{n}\times\boldsymbol{E}(\omega)=Z_s(\omega)\boldsymbol{n}\times\boldsymbol{n}\times\boldsymbol{H}(\omega)$, where $\boldsymbol{n}$ is the normal to the surface. The frequency dependent impedance function $Z_s(\omega)$ is represented by a general pole-residue expansion as

$$Z_s(\omega)=j\omega L+\alpha_0+\sum_{i=1}^{N_p}\frac{\alpha_i}{j\omega+\beta_i}. \tag{3}$$

In (3), α_i, β_i, and L are real coefficients and N_p is the order of the pole-residue model. Note that, the parameter L corresponds to the effective wall inductance which becomes particularly important for rough or oxidized surfaces at THz frequencies. In the numerical examples the surface impedance expansion order is taken N_p=*21*. According expansion coefficients where obtained by well-known vector fitting technique [4] in broad frequency range *f=100MHz-50THz* with sampling rate of *Δf=50MHz*. The fitting relative error below 1% was reached within the considered frequency range.

Following the procedure proposed in [5], the SIBC is written in the time domain as a set of ADEs,

$$\boldsymbol{n}\times\boldsymbol{E}=\left(\alpha_0+L\frac{\partial}{\partial t}\right)(\boldsymbol{n}\times\boldsymbol{n}\times\boldsymbol{H})+\alpha_0+\sum_{i=1}^{N_p}\boldsymbol{G}_i\,, \tag{4}$$

$$\frac{\partial\boldsymbol{G}_i}{\partial t}+\beta_i\boldsymbol{G}_i=\alpha_i(\boldsymbol{n}\times\boldsymbol{n}\times\boldsymbol{H}),\quad i=1,\ldots,N_p, \tag{5}$$

where $\boldsymbol{G}_i$ are auxiliary fields resembling effective magnetic currents on SIBC surfaces. Imposing (4) on SIBC surfaces and applying SFVTD discretization leads to a modified semi-discrete Faraday's law:

$$(\boldsymbol{M}_\mu+L\boldsymbol{A}_s)\frac{d\boldsymbol{h}}{dt}+\alpha_0\boldsymbol{A}_s\boldsymbol{h}=-\boldsymbol{C}\boldsymbol{e}-\boldsymbol{A}_s\sum_{i=1}^{N_p}\boldsymbol{g}_i\,, \tag{6}$$

$$\text{with}\quad \frac{\partial\boldsymbol{g}_i}{\partial t}+\beta_i\boldsymbol{g}_i=\alpha_i\boldsymbol{h},\quad i=1,\ldots,N_p, \tag{7}$$

where $\boldsymbol{g}_i$ are auxiliary degrees of freedom in the SFVTD sense, i.e. , corresponding to volume averages of the magnetic currents $\boldsymbol{G}_i$ on the face-staggered control volumes (cf. Fig. 1). The SIBC operator, $\boldsymbol{A}_s$, in (6) turns out to be a diagonal matrix with diagonal entries given by the mesh face areas for faces lying on a SIBC surface and zero otherwise.

TIME DISCRETIZATION

For the solution of (2), (6) and (7) in the time domain, the following time stepping strategy is applied. The discrete Ampere's and Faraday's equations, (2) and (6), respectively, are time-updated as usual using a leap-frog scheme. To preserve the stability bound of the original method, a semi-implicit approach is applied for the lossy SIBC term $\alpha_0\boldsymbol{A}_s\boldsymbol{h}$ appearing in (6) (cf. [6]). Finally, the set of ADEs (7) is solved with a second order accurate exponential time integrator [7]. The latter approach is known to provide optimal stability for stiff equations as is the case for the broadband SIBC-ADEs. Then, the overall time stepping scheme reads,

$$\boldsymbol{g}_0^n=\alpha_0\boldsymbol{h}^{n-1/2}, \tag{7}$$

$$\boldsymbol{g}_i^n=\boldsymbol{g}_i^{n-1}e^{-\beta_i\Delta t}+\frac{\alpha_i}{\beta_i}(1-e^{-\beta_i\Delta t})\boldsymbol{h}^{n-1/2}, \tag{8}$$

$$\boldsymbol{h}^{n+1/2}=\boldsymbol{h}^{n-1/2}-\Delta t\tilde{\boldsymbol{M}}_\mu^{-1}\left(\boldsymbol{C}\boldsymbol{e}^n+\boldsymbol{A}_s\sum_{i=0}^{N_p}\boldsymbol{g}_i^n\right), \tag{9}$$

$$\boldsymbol{e}^{n+1}=\boldsymbol{e}^n+\Delta t\boldsymbol{M}_\varepsilon^{-1}\left(\boldsymbol{C}^T\boldsymbol{h}^{n+1/2}-\boldsymbol{j}^{n+1/2}\right), \tag{10}$$

where a modified magnetic mass matrix $\tilde{\boldsymbol{M}}_\mu=\boldsymbol{M}_\mu+(L+\alpha_0\Delta t/2)\boldsymbol{A}_s$ is introduced. Note that $\tilde{\boldsymbol{M}}_\mu$ is diagonal, so that its inverse can be readily computed.

NUMERICAL RESULTS

As a first validation test for the method, a cubical copper resonator with side length *l=0.1mm* is considered. A TM_{211} -mode (λ=*81.65μm*, skin depth of δ=*34nm*) with *1J* energy is initially excited in the resonator. These are typical values for the short range wakefields in electron accelerators.

Since a closed form analytical solution is not known, the semi-analytical result [8] for the damping factor of lossy cavity modes is used as a reference for investigating the accuracy of the SIBC formulation. Figure 3 (top) shows the total electromagnetic energy decaying in the cavity as a function of time normalized to oscillation period *T≈0.27ps*. The numerical accuracy and convergence rate of the cavity filling time with respect to the mesh resolution Δ is shown in Fig. 3 (bottom). Second order convergence rate is observed.

Content from this work may be used under the terms of the CC BY 3.0 licence (© 2015). Any distribution of this work must maintain attribution to the author(s), title of the work, publisher, and DOI.

ISBN: 978-3-95450-168-7 doi:10.18429/JACoW-IPAC2015-MOPWA031

Content from this work may be used under the terms of the CC BY 3.0 licence (© 2015). Any distribution of this work must maintain attribution to the author(s), title of the work, publisher, and DOI.

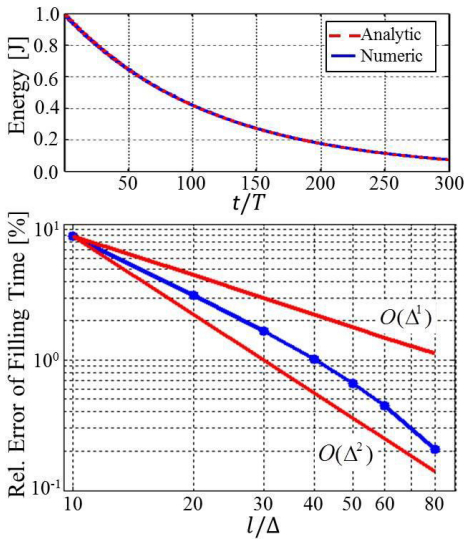

Figure 3: EM field energy vs. normalized time (top). Numerical convergence with respect to mesh resolution (bottom).

In next example the multimode excitation in a copper cubical resonator with side length *l=1cm* is considered. The resonant frequencies and according cavity filling times are presented in Table 1.

Table 1: Resonant Modes of Cubical Copper Cavity

Resonant Mode	Frequency [GHz]	Filling Time cτ [m]
TM_{111}	25.9628	1.1202
TM_{211}	36.7169	0.9420
TM_{311}	49.7150	0.8095
TM_{411}	63.5956	0.7157
TM_{511}	77.8884	0.6468

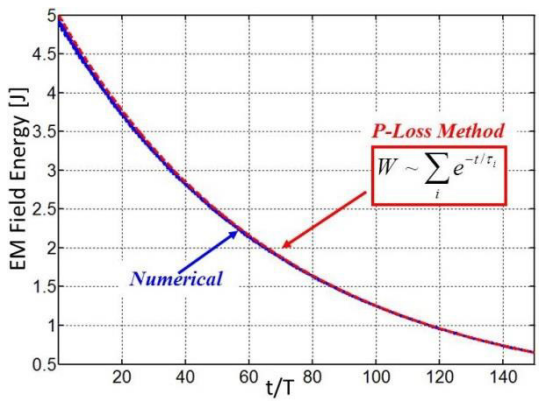

Figure 4: Total EM field energy decay obtained numerically (blue) and by power loss method (red).

Initially each of the modes are excited with *1J* energy. Figure 4 shows the total electromagnetic field energy decay in the cavity as a function of time normalized to oscillation period of the first mode *T≈38.5ps*. As can be seen already with mesh resolution *l/Δ=60* the numerical results are in good agreement with field energy decay obtained by power-loss method.

In all simulations, the maximum possible time step matching exactly the 1D-CFL stability limit is used.

CONCLUSION

The developed method is fully time domain and is dispersion free at magic time step. This results in large saving in computational time as well as improved accuracy. The resistive boundary model applies Surface Impedance Boundary Condition (SIBC) evaluation in time domain and covers boundary effects like frequency dependent conductivity, surface roughness and metal oxidation. The method was successfully tested and a good agreement between numerical simulation and perturbation theory is obtained. In addition the new method allows implementation of moving mesh approach that considerably reduces requirements on computational resources. The developed method will be implemented in PBCI code and will include moving mesh approach with parallel computation strategy. The code will be especially effective for short range wakefield calculations excited by ultra-short bunches in resistive structures.

REFERENCES

[1] K. L. Bane and G. Stupakov, "Resistive wall wakefield in the LCLS undulator beam pipe," SLAC, Stanford, CA, USA, Tech. Rep., 2004.

[2] E. Gjonaj, T. Lau, T. Weiland, and R. Wanzenberg, "Computation of short range wake field with PBCI", *ICFA Beam Dyn. Newslett.*, vol. 45, pp. 38–52, 2008.

[3] T. Lau, E. Gjonaj, and T. Weiland, *A Novel Staggered Finite Volume Time Domain Method*, ser. Mathematics in Industry. Springer-Verlag, Berlin/ Heidelberg, Germany, 2010, vol. 14, pp. 367–374.

[4] B. Gustavsen, "Improving the pole relocating properties of vector fitting", *IEEE Trans. on Power Delivery*, vol. 21, 2006, pp. 1587–1592.

[5] J. Woyna, E. Gjonaj, and T. Weiland, "Broadband surface impedance boundary conditions for higher order time domain discontinuous Galerkin method", COMPEL: The International Journal for Computation and Mathematics in Electrical and Electronic Engineering, vol. 33, no. 4, pp. 1082–1096, 2014.

[6] A. Taflove and S. Hagness, Computational Electrodynamics: The Finite-difference Time-domain Method, ser. Artech House antennas and propagation library. Artech House, 2005.

[7] A. Hochbruck and A. Ostermann, "Exponential integrators," Acta Numerica, vol. 19, pp. 209–286, May 2010.

[8] J. Gustincic, "A general power loss method for attenuation of cavities and waveguides," Microwave Theory and Techniques, IEEE Transactions on, vol. 11, no. 1, pp. 83–87, 1963.